How to cite: Urzică A., Mihu-Pintilie A., Stoleriu C. C., Lesenciuc D. C. (2024) Using 2D Hec-RAS Modeling for Modelling Major Flood Events (Post-2000) Downstream the Stânca Costești Reservoir (Middle Sector of Prut River). *2024 "Air and Water – Components of the Environment" Conference Proceedings*, Cluj-Napoca, Romania, p. 51-64, DOI: 10.24193/AWC2024_06.

USING 2D HEC-RAS MODELING FOR MODELLING MAJOR FLOOD EVENTS (POST-2000) DOWNSTREAM THE STÂNCA COSTEȘTI RESERVOIR (MIDDLE SECTOR OF PRUT RIVER)

ANDREI URZICĂ [1,2], ALIN MIHU-PINTILIE [1,3], CRISTIAN CONSTANTIN STOLERIU [1], DAN CRISTIAN LESENCIUC [1]

DOI: 10.24193/AWC2024_06

ABSTRACT. Using 2D Hec-RAS Modeling for Modelling Major Flood Events (Post-2000) Downstream the Stânca Costești Reservoir (Middle Sector of Prut River). Floods have been a significant concern for Romania, with notable events post-2000. These floods have been influenced by several factors, such as climate change, massive deforestation, inadequate urban planning and inadequate hydraulic infrastructure. The regions in the north-east of the country were particularly affected, suffering serious consequences for local communities, agriculture and infrastructure. The floods caused significant losses, including human and material losses. As main response, the Romanian authorities implemented 2007/60/EC Directive whose objective is to assess and manage major flood events. Considering the national legislation, the experiment consists in reconstructing the most destructive flood events which happened on Prut River. Along the Prut River, the most important flood events (post-2000) were recorded in 2005, 2008, 2010 and 2020. Using the HEC-RAS hydraulic modeling software, four different 2D hydraulic scenarios (2D-HS) were developed: 2D-HS1 (2005 flood event), 2D-HS2 (2008 flood event), 2D-HS3 (2010 flood event), 2D-HS4 (2020 flood event). Using the maximum flood extent, the total affected areas were extracted. The flood hazard was assessed by using the Australian Institute for Disaster Resilience (AIDR) methodology which use the Depth*Velocity (D*V) raster. The results shows that 497.7 km^2 were affected in the case of 2D-HS1, 569.3 km^2 were affected in the case of 2D-HS2, 553.4 km^2 were affected in the case of 2D-HS3 and 535.4 km^2 were affected in the case of 2D-HS4.

Keywords: flood modeling, 2D HEC-RAS, Prut River, hazard assessement

---

[1] Alexandru Ioan Cuza University of Iasi, Faculty of Geography and Geology, Department of Geography, Bd. Carol I 20A, 700505, Iasi, Romania. E-mail: urzica.andrei94@gmail.com, cristoan@yahoo.com, dlesenci@yahoo.com

[2] Research Center with Integrated Techniques for Atmospheric Aerosol Investigation in Romania, RECENT AIR, Laboratory of Interdisciplinary Research of Mountain Environment, Ion Gugiuman, Rarău Station for Research and Students Fellowships, 725100 Câmpulung-Moldovenesc, Suceava, România.

[3] Interdisciplinary Research Department, Field Science, Alexandru Ioan Cuza University of Iasi, St. Lascar Catargi 54, RO-700107 Iaşi, Romania. E-mail: mihu.pintilie.alin@gmail.com

1. INTRODUCTION

Worldwide, fluvial floods are the most spread and frequent natural disasters with the highest impact on human society. A combination of natural or anthropic conditions such as heavy rains, snowmelt, flow obstruction (e.g., ice jam) or dam failure are the main triggers of a catastrophic flood event (Adam et Nacu, 2020; Arghiuș et al., 2014; Enea et al., 2018; Huțanu et al., 2020; Liu et al., 2019; Van Alphen et al., 2009; Vasile et al., 2021; Romanescu et al., 2017a; Urzică et al., 2021; Yalcin, 2019). In the past few decades, these hydrological events are associated with climate changes due to the exponential increase in terms of frequency and magnitude. Through their spatial and temporal variability, floods can cause significant socio-economic and ecologic damages, loss of lives and landscape changes (Bomers et al., 2019). Despite the flood mitigation measures taken in the last few decades, annually, floods cause material damages of billions of US$ and thousands of fatalities. The developing areas are the most susceptible to be affected by floods as the world population continues to grow.

In Europe, in the last 100 years, the number of extreme flood events has increased. Romania, between 1985-2009, among other European countries (e.g., Czech Republic, Slovak Republic, United Kingdom, Germany and Austria) have faced the highest number of major flood events (Alfieri et al., 2015). Romania is hit by these extreme hydrological events either at the end of winter, as a result of the sudden melting of snow and heavy rains, or in the hot season, as a result of heavy rains (Romanescu et al., 2017b; Stoleriu et al., 2020; Dumitran et al., 2020; Corobov et al., 2021). The main cause of floods is the uncontrolled deforestation, especially in the mountainous areas (Peptenatu et al., 2020). The most devastating flood disasters which hit the Romanian territory are those from 1970, 1991, 2005, 2008, 2010 and 2020 (Mustățea, 2005; Chendeș, 2015). During these events, multiple casualties and billion-high (US$) material damages were recorded (Romanescu et al., 2011). Under the European Flood Directive (2007/60/EC), National Administration Romanian Waters (NARW) identified 3,150 km of river sectors with a high flood susceptibility.

Considering the above, this study consists in reconstructing the most destructive flood events which happened on Prut River middle floodplain. Along the Prut River, the most important flood events (post-2000) were recorded in 2005, 2008, 2010 and 2020. Using the HEC-RAS hydraulic modeling software, four different 2D hydraulic scenarios (2D-HS) were developed: 2D-HS1 (2005 flood event), 2D-HS2 (2008 flood event), 2D-HS3 (2010 flood event), 2D-HS4 (2020 flood event). For the 2D-HS1 we used the flow hydrograph recorded during the 2005 flood event, the land cover categories and the buildings extracted by digitizing the 2005 orthophotos edition; for 2D-HS2 we used the flow hydrograph recorded during the 2008 flood event, the land cover categories and the buildings extracted by digitizing the 2008 orthophotos edition; for 2D-HS3 we used the flow hydrograph recorded during the 2010 flood event, the land cover categories and the buildings extracted by digitizing the 2010 orthophotos edition; for 2D-HS4 we used the flow hydrograph recorded during the 2020 flood event, the land cover categories and the buildings extracted by digitizing the 2020 orthophotos edition. In order to highlight the floodplain response against major flood events, a comparison between the four 2D-HS in terms of land cover data and buildings was made. Furthermore, by using the methodology on hazard classification developed by the Australian Institute for Disaster Resilience (AIDR), the flood hazard severity was assessed.

2. DATA AND METHODS

2.1. Data used

2.1.1. Hydrological data – flood events

The Prut River has on the Romanian territory nine gauging stations, from the entry of Prut River to Prut-Danube confluence as follow: Oroftiana, Rădăuți-Prut, Stânca Aval, Ungheni, Prisăcani, Drânceni, Fălciu, Oancea and Șivița gauging stations (Fig. 1). For this experiment the Stânca Aval gauging station was used as a main gauging station. In order to capture the influence of the most important tributaries of Prut River on the flood extent, we used the hydrological data recorded at three secondary gauging stations: Ștefănești gauging station (Bașeu-Prut confluence), Victoria gauging station (Jijia-Prut River) and Iaşi gauging station (Bârlad-Prut confluence). The hydrological data (e.g., flow hydrograph, maximum flow discharge) used to develop the four 2D-HS was obtained from Prut-Bîrlad Water Basin Administration (PBWBA).

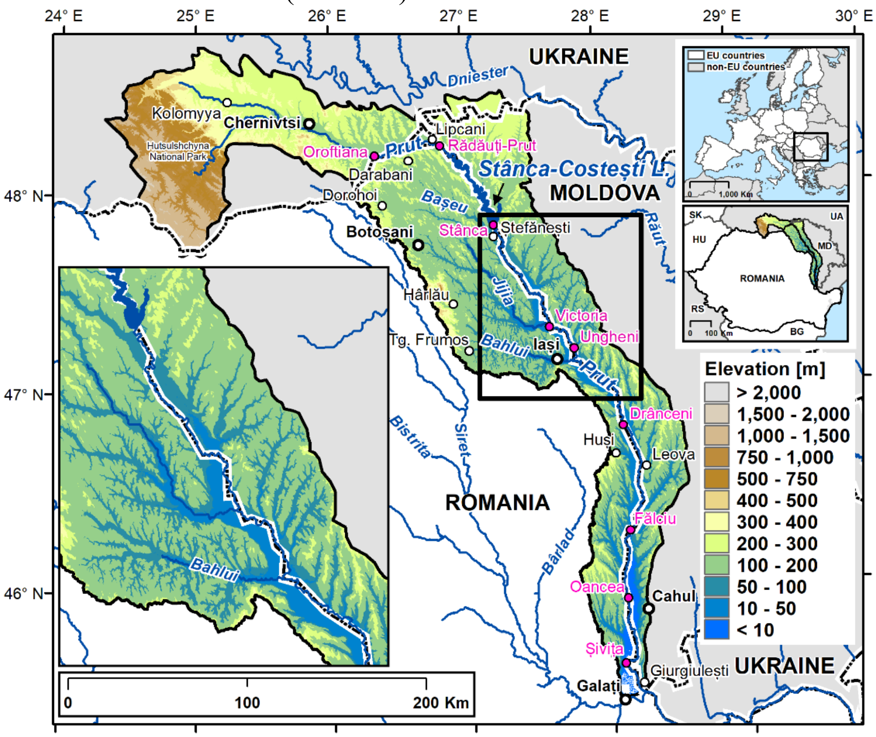

Fig. 1. Geographical location of the study area

Flood event: August 19 – 30, 2005

Due to heavy rains in the upper (Ukraine) and middle (Romania) Prut river basin, a historical flood event was recorded on Prut River (Enea et al., 2018). The flood event lasted 12 days, from 19 August to 30 August, 2005. The cumulative precipitation amounts from June-August exceeded 370 mm at Rădăuţi-Prut gauging station and 430 mm at Stânca Aval gauging station. A maximum flow rate of 2,640 m^3/s was recorded at Rădăuţi-Prut gauging station, on 21 August and a maximum flow rate of 570 m^3/s at Stânca Aval gauging station, on 22 August. The flow rate recorded in August 2008 is the fourth from Prut River history. The historical flow rate recorded at Rădăuţi-Prut gauging station was exceeded by the flood event recorded in 2008 and 2020. No casualties were recorded on Romanian territory during the flood event.

Flood event: July 19 – August 23, 2008

The historical flood event recorded in 2008 on Prut River which started on 19 July and lasted 31 days, is the most catastrophic hydrological event from Prut River history. Due to a high amount of precipitation with torrential character on the upper (Ukraine) and middle (Romania) Prut river basin (162 mm in 30 days at Rădăuţi-Prut gauging station), a historical flow of 4,240 m^3/s was recorded at Rădăuţi-Prut gauging station and 1,260 m^3/s at Stânca Aval gauging station (Romanescu et al., 2011; Romanescu & Stoleriu, 2017a). The important role of Stânca-Costeşti reservoir in flood mitigation is proved by the limited damages recorded downstream of the lake. The most important damages were recorded upstream of Stânca-Costeşti reservoir: 1,500 ha arable land flooded, 500 ha pastures and grassland flooded, 380 ha forest flooded, 64 households flooded, 170 households completely destroyed, 220 wells infected, more than 300 bridges destroyed. No casualties were recorded on Romanian territory during the flood event (Romanescu et al., 2011, 2017a).

Flood event: June 23 – July 27, 2010

The flood event which started on 23 June on Prut River lasted 35 days. This flood event which had as trigger mechanism the heavy rains recorded in the upper and middle Prut river basis is classed as fourth in terms of recorded maximum flow rate. The cumulative heavy rains from May-July (454 mm in 90 days at Rădăuţi-Prut gauging station) on the upper (Ukraine) and middle (Romania) Prut river basin caused a maximum flow rate of 2,310 m^3/s at Rădăuţi-Prut gauging station. Due to the controlled outflow of Stânca-Costeşti reservoir a maximum flow rate of 885 m^3/s was recorded at Stânca Aval gauging station (Romanescu & Stoleriu, 2017a). No casualties were recorded on Romanian territory during the flood event.

Flood event: June 16 – July 5, 2020

The flood event which started on 16 June and ended on 5 July is the second most catastrophic hydrological event recorded on Prut River. The flood event was triggered by heavy rains from the upper (Ukraine) and middle (Romania) Prut river basin. The heavy rains on Ukrainian territory caused the failure of several dam reservoirs which increased the flow rate of Prut River. At Rădăuţi-Prut gauging station no precipitation data were recorded, instead at Oroftiana gauging station (located at entry of Prut River on Romanian territory) a total of 180 mm were recorded in 35 days. In the same period (35 days) the amount of precipitation recorded at Stânca Aval gauging station exceeded 90 mm. At Rădăuți-Prut gauging station a maximum flow rate of 2,965 m^3/s was recorded, on 26 June and 848 m^3/s at Stânca Aval gauging station, on 27 June. No casualties were recorded on Romanian territory during the flood event.

2.1.2. LiDAR-derived DTM data

The products derived from LiDAR data, especially Digital Surface Model (DSM) and Digital Terrain Model (DTM) can offer a high understanding of the hydrological processes and also a real improvement of the hydrological and hydraulic modeling. PBWBA through the SMIS-CSNR No.17945 project: Works to reduce the flood risk in the Prut-Bîrlad River Basin (PBRB) were able to acquire for the total area which is under its administration (20,570 km^2) LiDAR products (DSM, DTM). Within the project a detailed flight using a Leica ALS60 Airborne Laser Scanner (ALS) was made. The detailed flight altitude granted a point cloud density of 2-3 points/m^2. Based on geostatistical interpolation methods, more than 87,000 raster files (.tiff files) were obtained. For our study area, we processed 5,500 raster files (.tiff files) using a raster dataset (Stoleriu et al., 2020, Huțanu et al., 2020) Additionally, in order to capture the impact of the solid object given by the presence of buildings (e.g., houses, attachment buildings, administrative or industrial buildings) on hydraulic modeling, they were integrated in the final LiDAR-derived DTM (Urzică et al., 2021, Ciurte et al., 2023). Four buildings databases were obtained by digitizing the orthophotos collected in 2005, 2008, 2010 and 2020. In order to integrate the buildings in the LiDAR-derived DTM, a height of 6 m was assigned to each building, rasterized and joined with the LiDAR-derived DTM in a raster dataset (Urzică et al., 2021). Thus, four different LiDAR-derived DTM were created based on the initial LiDAR-derived DTM and the digitized buildings from orthophotos (2005, 2008, 2010 and 2020 edition).

2.2. Methods

2D HEC-RAS streamflow modeling

In order to generate the flood extent and the flood hazard maps for the most important flood events which occurred on Prut River, four 2D-HS were developed by using the new version of HEC-RAS hydraulic modeling software (v. 5.0.7.). With the new version of the software, all the necessary geometries and the improvement of the hydraulic model were created in the RAS Mapper module. To develop the four 2D-HS, an initial hydraulic model whose geometries remained unchanged, was created. To create the initial hydraulic model a 2D flow area was established as a general floodable area (74,248 ha). Using a computation point spacing of 15 m, a polygonal mesh with more than 3,300,000 cells was generated. A cell size of 15x15 m was chosen due to the small variations of the water surface elevation on the Prut floodplain. For the areas where rapid changes on water elevation can occur, we choose to refine the created mesh using break lines and refinement regions (Brunner, 2016, 2020). The breaklines (polylines) were used for the top of the levees and the refinement regions (polygonal areas) for the main channel of Prut River and the confluence section of Prut River with its tributaries (Bașeu, Jijia, Bârlad rivers). A cell size of 5x5 m was set for each breakline and refinement region. Using the initial hydraulic model, for each 2D-HS, 2D-HS1 (2005 flood event), 2D-HS2 (2008 flood event), 2D-HS3 (2010 flood event), 2D-HS4 (2020 flood event), which represent a recorded flood event, a different LiDAR-derived DTM, roughness coefficient and a flow hydrograph corresponding to the flood event years were used.

HEC-RAS software can perform a 2D unsteady flow analysis using two different equations: (1) the 2D Full Saint Venant equation and (2) & (3) 2D Diffusion wave equation. In order to choose what equation is more appropriate to our analysis two different hydraulic models with 2D Full Saint Venant equation and 2D Diffusion wave equation were created and compared. If the differences between the two hydraulic models are not significant, the user can proceed with the 2D Diffusion wave equation (Brunner, 2016, 2020). Thereby, for each 2D-HS the analysis was completed using Equation (2) and (3).

$$\frac{\partial \zeta}{\partial t} + \frac{\partial p}{\partial x} + \frac{\partial q}{\partial y} = 0 \quad (1)$$

$$\frac{\partial p}{\partial t} + \frac{\partial}{\partial x}\left(\frac{p^2}{h}\right) + \frac{\partial}{\partial y}\left(\frac{pq}{h}\right) = -\frac{n^2 pg\sqrt{p^2+q^2}}{h^2} - gh\frac{\partial \zeta}{\partial x} + pf + \frac{\partial}{\rho \partial x}(h\tau_{xx}) + \frac{\partial}{\rho \partial y}(h\tau_{xy}) \quad (2)$$

$$\frac{\partial q}{\partial t} + \frac{\partial}{\partial y}\left(\frac{q^2}{h}\right) + \frac{\partial}{\partial x}\left(\frac{pq}{h}\right) = -\frac{n^2 qg\sqrt{p^2+q^2}}{h^2} - gh\frac{\partial \zeta}{\partial y} + qf + \frac{\partial}{\rho \partial y}(h\tau_{yy}) + \frac{\partial}{\rho \partial x}(h\tau_{xy}) \quad (3)$$

Where: h is the water depth (m), p and q are the specific flow in the x and y directions (m^2s^{-1}), ζ is the surface elevation (m), g is the acceleration due to gravity (ms^{-2}), n is the Manning resistance, ρ is the water density (kg m^{-3}), τ_{xx}, τ_{yy}, and τ_{xy} are the components of the effective shear stress and f is the Coriolis (s^{-1}). When the diffusive wave is selected the inertial terms of the momentum equations are neglected (Equations (2) and (3)).

To prevent the instability of the hydraulic model, the computational time was estimated using the Courant condition (Equation 4). Because the four 2D-HS are similar in terms of input data, a time step of 30 second was used for each 2D-HS. To run each 2D-HS, the model took between 24–36 h to complete the simulation.

$$C = \frac{V_w \Delta T}{\Delta X} \leq 1; \quad \Delta T = \frac{\Delta x}{V_w}; \quad V_w = \frac{dQ}{dA} \quad (4)$$

Where: C is the Courant number, ΔT is the time step (seconds), Δx is the distance step in meters (average two-dimensional cell size), V_w is the flood wave speed (m/s), dQ is the change in discharge over a short time interval ($Q_2 - Q_1$), dA is the change in cross section area over a short time interval ($A_2 - A_1$).

Land cover data

The land cover polygon features were obtained by using on-screen digitizing techniques. Considering the importance of the roughness coefficient in hydraulic modeling, the land cover data was obtained according to the flood event year. Thereby, using the orthophotos from 2005, 2008, 2010 and 2020 and Corine Land Cover classifications, seven land cover categories were identified in the Prut River floodplain and the roughness coefficient values were set as follow: discontinuous urban fabric (0.2), pastures (0.035), annual crops associated with permanent crops (0.035), broad-leaved forest (0.1), transitional woodland-shrub (0.06), inland marshes (0.07) and water courses (0.013) (Brunner, 2020; Mihu-Pintilie et al., 2019, Urzică et al., 2021).

Flood hazard assessment

The flood hazard was assessed using the AIDR methodology which use the Depth*Velocity (D*V) rasters and consists in six flood hazard categories: H1 (D*V ≤ 0.3 m^2/s), H2 (D*V range between >0.3 m^2/s and ≤ 0.6 m^2/s), H3 (D*V range between >0.6 m^2/s and ≤ 1.2 m^2/s), H4 (D*V range between > 1.2 m^2/s and $\leq$ 2 m^2/s), H5 (D*V range between >2 m^2/s and ≤ 4 m^2/s), H6 (D*V> 4 m^2/s) (Table 1) (AIDR, 2017; Urzică et al., 2021).

Table 1. ***Flood hazard classification based on the flood depth and flood velocity according to the AIDR (AIDR, 2017)***

Flood Hazard	D*V (m^2/s)	Hazard Description
H1	≤ 0.3	Generally sage vehicles, people and buildings
H2	>0.3 ≤ 0.6	Unsafe for small vehicles
H3	>0.6 ≤ 1.2	Unsafe for vehicles, children and the elderly
H4	>1.2 ≤ 2	Unsafe for vehicles and people
H5	>2 ≤ 4	Unsafe for vehicles and people. All the building types vulnerable to structural damage. Some less robust building types vulnerable to failure
H6	> 4	Unsafe for vehicles and people. All building types considered vulnerable to failure.

3. RESULTS

Floodplain response during the major flood events

Using the maximum flood extent, the total affected areas were extracted. The results show that 497.7 km^2 were affected in the case of 2D-HS1, 569.3 km^2 were affected in the case of 2D-HS2, 553.4 km^2 were affected in the case of 2D-HS3 and 535.4 km^2 were affected in the case of 2D-HS4 (Fig. 2, Table 2).

2D-HS1 (flood event: August 19 – 30, 2005)

According to 2D-HS1 results, a total surface of 497.7 km^2 was affected. In terms of affected land use categories, 38.7% (192.8 km^2) are annual crops associated with permanent crops, 29.1% (144.6 km^2) are pastures, 18.9% (94.2

km^2) are broad-leaved forest, 6.9% (34.3 km^2) are water courses, 4.6% (22.8 km^2) are discontinuous urban fabric, 1.2% (5.8 km^2) are inland marshes and 0.6% (3.1 km^2) are transitional woodland-shrubs (Table 2). Based on the flood hazard classification, 88.1% (438.4 km^2) of the total affected area are in the H1 class (≤ 0.3 m^2/s), 5.3% (26.4 km^2) in the H2 class (≤0.6 m^2/s), 2.4% (11.7 km^2) in the H3 class (≤1.2 m^2/s), 1.2% (6.0 km^2) in the H4 class (≤2 m^2/s), 2.4% (11.7 km^2) in the H5 class (≤4 m^2/s) and 0.7% (3.4 km^2) in the H6 class (>4 m^2/s) (Table 3). Regarding the discontinuous urban fabric, out of the total of 88 settlements within the study area, 67 settlements were affected by floods (16 settlements were entirely covered by waters). Within the 67 settlements, 7,597 buildings were affected by floods, of which 98.6% (7,490 buildings) are in the H1 class (≤ 0.3 m^2/s), 0.9% (68 buildings) in the H2 class (≤0.6 m^2/s), 0.4% (32 buildings) in the H3 class (≤1.2 m^2/s) and 0.1% (7 buildings) in the H4 class (≤2 m^2/s) (Table 3).

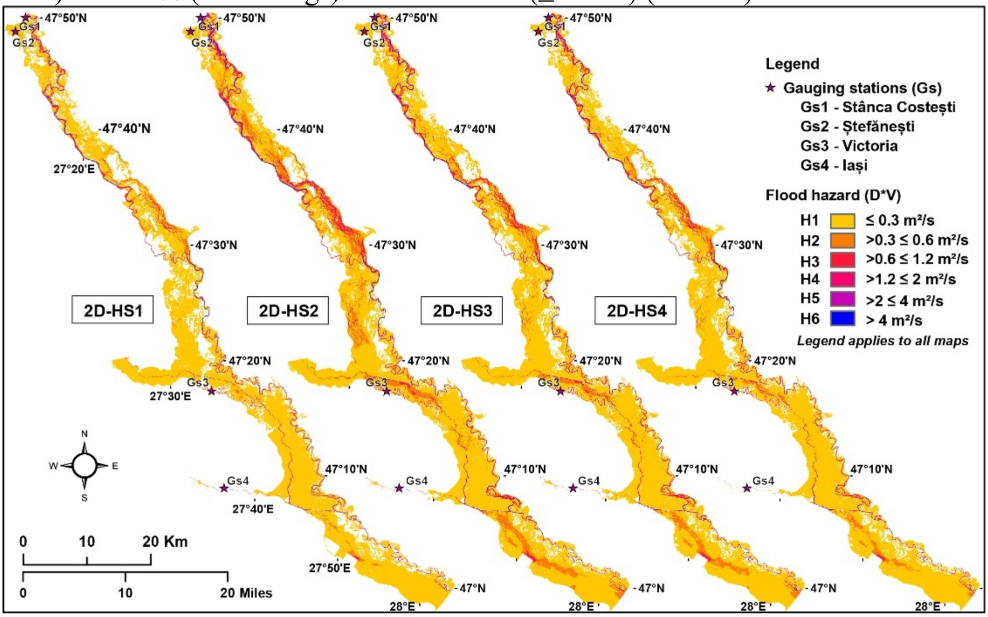

Fig. 2. 2D HEC-RAS flood scenarios

Table 2. *Affected land use categories according to each 2D HEC-RAS scenarios*

2D-HS2 (flood event: July 19 – August 23, 2008)

According to 2D-HS2 results, 569.3 km^2 were affected by floods. In terms of affected land use categories, 40.9% (233.0 km^2) are annual crops associated with permanent crops, 26.5% (150.9 km^2) are pastures, 18.9% (107.7 km^2) are broad-leaved forest, 6.7% (38.1 km^2) are water courses, 4.9% (28.0 km^2) are discontinuous urban fabric, 1.6% (9.3 km^2) are inland marshes and 0.4% (2.4 km^2) are transitional woodland-shrubs (Table 2).

Label 3 CLC	Land use categories							
	2D-HS1		2D-HS2		2D-HS3		2D-HS4	
	(km^2)	(%)	(km^2)	(%)	(km^2)	(%)	(km^2)	(%)
Discontinuous urban fabric	22.8	4.6	28.0	4.9	22.2	4.0	20.6	3.8
Pastures	144.6	29.1	150.9	26.5	140.2	25.3	136.8	25.6
Annual crops associated with permanent crops	192.8	38.7	233.0	40.9	246.3	44.5	238.1	44.5
Broad-leaved forest	94.2	18.9	107.7	18.9	102.5	18.5	98.7	18.4
Transitional woodland-shrub	3.1	0.6	2.4	0.4	3.8	0.7	3.3	0.6
Inland marshes	5.8	1.2	9.3	1.6	3.6	0.6	2.7	0.5
Water courses	34.3	6.9	38.1	6.7	34.8	6.3	35.2	6.6
Total	**497.7**	100	**569.3**	100	**553.4**	100	**535.4**	100

Table 3. ***Flood hazard classification for 2D-HS1 (flood event: August 19 – 30, 2005)***

Flood Hazard	D*V (m^2/s)	Surface (km^2)	Surface (%)	Buildings (No.)	Buildings (%)
H1	≤ 0.3	438.4	88.1	7,490	98.6
H2	>0.3 ≤ 0.6	26.4	5.3	68	0.9
H3	>0.6 ≤ 1.2	11.7	2.4	32	0.4
H4	>1.2 ≤ 2	6.0	1.2	7	0.1
H5	>2 ≤ 4	11.7	2.4	-	-
H6	> 4	3.4	0.7	-	-

Based on the flood hazard classification, 75.7% (431.2 km^2) of the total affected area are in the H1 class (≤ 0.3 m^2/s), 14.8% (84.4 km^2) in the H2 class (≤0.6 m^2/s), 4.8% (27.3 km^2) in the H3 class (≤1.2 m^2/s), 1.7% (9.7 km^2) in the H4 class (≤2 m^2/s), 2.0% (11.6 km^2) in the H5 class (≤4 m^2/s) and 0.9% (5.1 km^2) in the H6 class (>4 m^2/s) (Table 4).

Table 4. ***Flood hazard classification for 2D-HS2 (flood event: July 19 – August 23, 2008)***

Flood Hazard	D*V (m^2/s)	Surface (km^2)	Surface (%)	Buildings (No.)	Buildings (%)
H1	≤ 0.3	431.2	75.7	10,922	95.73
H2	>0.3 ≤ 0.6	84.4	14.8	438	3.84
H3	>0.6 ≤ 1.2	27.3	4.8	39	0.34
H4	>1.2 ≤ 2	9.7	1.7	7	0.06
H5	>2 ≤ 4	11.6	2.0	3	0.03
H6	> 4	5.1	0.9	-	-

A number of 75 settlements were affected (16 settlements were entirely covered by waters). Within the 75 settlements, a total number of 11,409 buildings were affected by floods, of which 95.7% (10,922 buildings) are in the H1 class (≤ 0.3 m^2/s), 3.84% (438 buildings) in the H2 class (≤0.6 m^2/s), 0.34% (39 buildings) in the H3 class (≤1.2 m^2/s), 0.06% (7 buildings) in the H4 class (≤2 m^2/s) and 0.03% (3 buildings) in the H5 class (≤4 m^2/s) (Table 4).

2D-HS3 (flood event: June 23 – July 27, 2010)

According to 2D-HS3 results, a surface 553.4 km^2 was affected by floods. In terms of affected land use categories, 44.5% (246.3 km^2) are annual crops associated with permanent crops, 25.3% (140.2 km^2) are pastures, 18.5% (102.5 km^2) are broad-leaved forest, 6.3% (34.8 km^2) are water courses, 4.0% (22.2 km^2) are discontinuous urban fabric, 0.7% (3.8 km^2) are transitional woodland-shrubs and 0.6% (3.6 km^2) are inland marshes (Table 2). Based on the flood hazard classification, 81.7% (451.9 km^2) of the total affected area are in the H1 class (≤ 0.3 m^2/s), 10.5% (58.3 km^2) in the H2 class (≤0.6 m^2/s), 3.5% (19.5 km^2) in the H3 class (≤1.2 m^2/s), 1.3% (7.4 km^2) in the H4 class (≤2 m^2/s), 2.1% (11.5 km^2) in the H5 class (≤4 m^2/s) and 0.9% (4.8 km^2) in the H6 class (>4 m^2/s) (Table 5). A number of 74 settlements were affected (16 settlements were entirely covered by waters). Within the 74 settlements, a total number of 10,679 buildings were affected by floods, of which 97.03% (10,362 buildings) are in the H1 class (≤ 0.3 m^2/s), 2.58% (275 buildings) in the H2 class (≤0.6 m^2/s), 0.32% (34 buildings) in the H3 class (≤1.2 m^2/s), 0.06% (6 buildings) in the H4 class (≤2 m^2/s) and 0.02% (2 buildings) in the H5 class (≤4 m^2/s) (Table 5).

Table 5. ***Flood hazard classification for 2D-HS3 (flood event: June 23 – July 27, 2010)***

Flood Hazard	D*V (m^2/s)	Surface (km^2)	Surface (%)	Buildings (No.)	Buildings (%)
H1	≤ 0.3	451.9	81.7	10,362	97.03
H2	>0.3 ≤ 0.6	58.3	10.5	275	2.58
H3	>0.6 ≤ 1.2	19.5	3.5	34	0.32
H4	>1.2 ≤ 2	7.4	1.3	6	0.06
H5	>2 ≤ 4	11.5	2.1	2	0.02
H6	> 4	4.8	0.9	-	-

2D-HS4 (flood event: June 16 – July 5, 2020)

According to 2D-HS4 results, a surface 535.4 km^2 was affected by floods. In terms of affected land use categories, 44.5% (238.1 km^2) are annual crops associated with permanent crops, 25.6% (136.8 km^2) are pastures, 18.4% (98.7 km^2) are broad-leaved forest, 6.6% (35.2 km^2) are water courses, 3.8% (20.6 km^2) are discontinuous urban fabric, 0.6% (3.3 km^2) are transitional woodland-shrubs and 0.5% (2.7 km^2) are inland marshes (Table 2). Based on the flood hazard classification, 84.5% (452.3 km^2) of the total affected area are in the H1 class (≤

0.3 m^2/s), 8.1% (43.6 km^2) in the H2 class (≤0.6 m^2/s), 3.2% (17.0 km^2) in the H3 class (≤1.2 m^2/s), 1.2% (6.7 km^2) in the H4 class (≤2 m^2/s), 2.2% (11.6 km^2) in the H5 class (≤4 m^2/s) and 0.8% (4.3 km^2) in the H6 class (>4 m^2/s) (Table 6). A number of 69 settlements were affected (16 settlements were entirely covered by waters). Within the 69 settlements, a total number of 9,690 buildings were affected by floods, of which 97.21% (9,420 buildings) are in the H1 class (≤ 0.3 m^2/s), 2.43% (236 buildings) in the H2 class (≤0.6 m^2/s), 0.28% (28 buildings) in the H3 class (≤1.2 m^2/s) and 0.06% (6 buildings) in the H4 class (≤2 m^2/s) (Table 6).

Table 6. ***Flood hazard classification for 2D-HS4 (flood event: June 16 – July 5, 2020)***

Flood Hazard	D*V (m^2/s)	Surface (km^2)	Surface (%)	Buildings (No.)	Buildings (%)
H1	≤ 0.3	452.3	84.5	9420	97.21
H2	>0.3 ≤ 0.6	43.6	8.1	236	2.43
H3	>0.6 ≤ 1.2	17.0	3.2	28	0.28
H4	>1.2 ≤ 2	6.7	1.2	6	0.06
H5	>2 ≤ 4	11.6	2.2	-	-
H6	> 4	4.3	0.8	-	-

4. DISCUSSIONS

In accordance with the European Flood Directive 2007/60/EC, which requires the creation of risk maps, hazard maps and flood risk management plans for each member state of the European Union, Romania generated flood hazard maps based on mathematical modeling (both 1D and 2D) for various recurrence probabilities (e.g., 0.1%, 1%, and 3%). Although the Prut River constitutes the natural border between Romania and the Republic of Moldova, flood hazard maps were not generated for the Prut River in the initial phase of the project.

A joint effort between the two countries was only initiated in 2017 through the EASTAVERT PROJECT 'The prevention and protection against floods in the upper Siret and Prut River Basins, through the implementation of a modern monitoring system with automatic stations" where risk and hazard maps were generated for the entire floodplain of the Prut River. Within this project, the calculation of maximum discharges for different probabilities of flood occurrence was based on historical discharge data recorded at Prut River gauging stations. Therefore, we were able to compare the results obtained in our study with those obtained in the aforementioned project.

Although there is currently a flood risk management plan, as well as individual studies that rely on hydraulic modeling along the Prut River, a comprehensive study conducting a quantitative analysis of damages, both in Romanian territory and in the Republic of Moldova, has not been conducted.

Paradoxically, the access to high-accuracy data (e.g., LiDAR-derived DEM) constitutes the limitations of this study. The main limitation is the lack of infrastructure for processing a very large volume of data, which is why only the middle sector of the Prut River was considered for hydraulic modeling.

5. CONCLUSIONS

In this study, 2D HEC-RAS hydraulic modeling and high-density LiDAR data were utilized to reconstruct the most destructive flood events occurring on the middle floodplain of the Prut River post-2000. Four distinct 2D hydraulic scenarios (2D-HS) were developed for this purpose: 2D-HS1 (2005 flood event), 2D-HS2 (2008 flood event), 2D-HS3 (2010 flood event), and 2D-HS4 (2020 flood event). The outcomes regarding the impact of each flood event can be summarized as follows:

- Flood extent: The results indicate that 497.7 km^2 were affected in the case of 2D-HS1, 569.3 km^2 in 2D-HS2, 553.4 km^2 in 2D-HS3, and 535.4 km^2 in 2D-HS4.
- Habitation area affected: the outcomes show that 67 settlements (7,597 buildings affected) were impacted by floods in 2D-HS1, 75 settlements (11,409 buildings affected) in 2D-HS2, 74 settlements (10,679 buildings affected) in 2D-HS3, and 69 settlements (9,690 buildings affected) in 2D-HS4.
- Flood hazard assessment using AIDR methodology: The most destructive flood event occurred in 2008, with 95.7% (10,922 buildings) falling into the H1 class ($\leq$ 0.3 m^2/s), 3.84% (438 buildings) in the H2 class ($\leq$ 0.6 m^2/s), 0.34% (39 buildings) in the H3 class ($\leq$ 1.2 m^2/s), 0.06% (7 buildings) in the H4 class ($\leq$ 2 m^2/s), and 0.03% (3 buildings) in the H5 class ($\leq$ 4 m^2/s).

Compared to 1D hydraulic models 2D hydraulic models provide a more accurate representation within a floodplain. Having the ability to manage complex geometries such as bridges, embankments, irregular networks of polygons with high resolution, products such as flood velocity, water depth, water recession, water duration, can be generated. Based on these products generated in the RAS Module, complex analyses can be conducted, and correlating them with local climatic conditions can lead to identifying patterns in flood occurrence, thus contributing to adjusting and improving flood management plans.

Based on the aforementioned, developing streamflow scenarios in highly vulnerable areas like the middle Prut floodplain is a crucial aspect of any flood mitigation effort. In this context, the 2D streamflow hydraulic model proposed in this study demonstrates that the method can become a valuable asset in flood mitigation and future flood hazard management in the region.

REFERENCES

1. Adam, B.O., Nacu, S. (2020), Flood Events in Bacău County During 2005-2019. 2020 ”Air and Water – Components of the Environment” Conference Proceedings, Cluj-Napoca, Romania, p. 59-70, DOI:10.24193/AWC2020_06.

2. AIDR (Australian Institute for Disaster Resilience) (2017), Australian Disaster Resilience Handbook 7 Managing the Floodplain: A Guide to Best Practice in Flood Risk Management in Australia. Available online: http://www.dpmc.gov.au/government/its-honour. Accessed on 10.11.2023
3. Alfieri, L., Feyen, L., Dottori, F., & Bianchi A. (2015), Ensemble flood risk assessment in Europe under high end climate scenarios. Global Environemnt Change, 55, 199-212. DOI:10.1016/j.gloenvcha.2015.09.004.
4. Arghiuş, V., Ozunu, A., Samara, I., & Roşian, G. (2014), Results of the post flash-flood disaster investigations in the Transylvanian Depression (Romania) during the last decade (2001–2010), Natural Hazards and Earth System Sciences, 14, 535–544, DOI:10.5194/nhess-14-535-2014.
5. Bomers, A., Van der Meulen, B., Schielen R.M.J., & Hulscher, S.J.M.H. (2019), Historic flood reconstruction with the use of an Artificial Neural Network. Water Resources Research, 55, 9673-9688. DOI:10.1029/2019WR025656.
6. Brunner G.W. (2016), CEIWR-HEC. HEC-RAS River Analysis System, 2D Modeling User's Manual; Version 5.0. Available online: https://www.hec.usace.army.mil/software/hec-ras/documentation. Accessed on 05.10.2023
7. Brunner G.W. (2020), CEIWR-HEC. HEC-RAS River Analysis System, 2D Modeling User's Manual; Version 6.0. Available online: https://www.hec.usace.army.mil/software/hec-ras/documentation. Accessed on 05.10.2023.
8. Ciurte, D.L., Mihu-Pintilie, A., Urzică, A., Grozavu, A. (2023), Integrating LiDAR data, 2D HEC-RAS modeling and Remote Sensing to develop flood hazard maps downstream of a large reservoir in the Inner Eastern Carpathians. Carpathian Journal of Earth and Environmental Sciences, 18(1), 149 – 169. DOI: 10.26471/cjees/2023/018/248.
9. Chendeș, V., Bălteanu, D., Micu, D., Sima, M., Ion, B., Grigorescu, I., Persu, M., & Dragotă C. (2015), A database design of major past flood events in Romania from national and international inventories. Air and Water – Components of the Environment Conference Proceedings, 7, 25-32. DOI:10.17378/AWC2015_04.
10. Corobov R., Ene A., Trombitsky I. & Zubcov E. (2021), The Prut River under climate change and hydropower impact. Sustainability, 13(1), 66. DOI: https://doi.org/10.3390/su13010066.
11. Dumitran G.E., Vuta L.I., Popa B. & Popa F. (2020), Hydrological variability impact on eutrophication in a large Romanian border reservoir, Stânca-Costești. Water 12(11), 3065. DOI: https://doi.org/10.3390/w12113065.
12. Enea A., Urzică A. & Breabăn I.G. (2018), Remote Sensing, GIS and HEC-RAS techniques, applied for flood extent validation, based on Landsat Imagery, LiDAR and hydrological data. Case study: Baseu River, Romania. Journal of Environmental Protection and Ecology, 19(3), 1091–1101.
13. Huţanu E., Mihu-Pintilie A. Urzică A., Paveluc, L.E., Stoleriu C.C. & Grozavu A. (2020), Using 1D HEC-RAS Modeling and LiDAR Data to Improve Flood Hazard Maps Accuracy: A Case Study from Jijia Floodplain (NE Romania). Water, 12(6), 1624. DOI: https://doi.org/10.3390/w12061624.
14. Liu, Z., Merwade, V., & Jafarzadegan, K. (2019). Investigating the role of model structure and surface roughness in generating flood inundation extents using one- and two- dimensional hydraulic models. Journal of Flood Risk Management, 12:e12347. DOI:10.1111/jfr3.12347.

15. Mihu-Pintilie A., Cîmpianu C.I., Stoleriu C.C., Pérez M.N. & Paveluc L.E. (2019), Using High-Density LiDAR Data and 2D Streamflow Hydraulic Modeling to Improve Urban Flood Hazard Maps: A HEC-RAS Multi-Scenario Approach. Water, 11(9), 1832. DOI: https://doi.org/10.3390/w11091832.
16. Mustățea, A. (2005), Exceptional floods on the Romania territory. Genesis and effects. Onesta 94.
17. Peptenatu, D., Grecu, A., Simion A.G., Gruia, K.A., Andronache, I., Draghici, C.C., & Diaconu D.C. (2020), Deforestation and frequency of floods in Romania. In A. Negm, G. Romanescu, & M. Zelenakova (Eds.), Water resources management in Romania (pp. 279– 306). Switzerland: Springer Water.
18. Romanescu G., Stoleriu C.C. & Romanescu A.M. (2011), Water reservoirs and the risk of accidental flood occurrence. Case study: Stânca–Costești reservoir and the historical floods of the Prut river in the period July–August 2008, Romania. Hydrological Processes, 25(13), 2056–2070. DOI: https://doi.org/10.1002/hyp.7957.
19. Romanescu G. & Stoleriu C.C. (2017a), Exceptional floods in the Prut basin, Romania, in the context of heavy rains in the summer of 2010. Natural Hazards and Earth System Sciences, 17(3), 381–396. DOI: https://doi.org/10.5194/nhess-17-381-2017.
20. Romanescu G., Cîmpianu C.I., Mihu-Pintilie A. & Stoleriu C.C. (2017b), Historic flood events in NE Romania (post-1990). Journal of Maps, 13(2), 787–798. DOI: https://doi.org/10.1080/17445647.2017.1383944.
21. Stoleriu C.C., Urzică A., & Mihu-Pintilie A. (2020), Improving flood risk map accuracy using high-density LiDAR data and the HEC-RAS river analysis system: A case study from north-eastern Romania. Journal of Flood Risk Management, 13(1). DOI: https://doi.org/10.1111/jfr3.12572.
22. Urzică A., Mihu-Pintilie A., Stoleriu C.C., Cîmpianu C.I., Huțanu E., Pricop C.I. & Grozavu A. (2021), Using 2D HEC-RAS modeling and embankment dam break scenario for assessing the flood control capacity of a multi-reservoir system (NE Romania). Water, 13(1), 57. DOI: https://doi.org/10.3390/w13010057.
23. Van Alphen, J., Martini, F., Loat, R., Slomp, R., & Passchier, R. (2009), Flood risk mapping in Europe, experiences and best practices. Journal of Flood Risk Management, 2(4), 285-292. DOI:10.1111/j.1753-318X.2009.01045.x
24. Vasile, D.M., Popa, M.C., Toma, F., Diaconu, D.C. (2021), Flash Flood Assessment Using GIS and the Frequency Ratio Bivariate Statistical Model – Case Study, Codlea, Romania. 2021 ”Air and Water –Components of the Environment” Conference Proceedings, Cluj-Napoca, Romania, p. 61-74, DOI:10.24193/AWC2021_06.
25. Yalcin, E. (2019), Two-dimensional hydrodynamic modelling for urban flood risk assessment using unmanned aerial vehicle imagery: A case study of Kirsehir, Turkey. Journal of Flood Risk Management, 12 (Suppl.1):e12499. DOI:10.1111/jfr3.12499